

# Synthesis and Preliminary Evaluation of $^{11}\text{C}$ -Labeled VU0467485/AZ13713945 and Its Analogues for Imaging Muscarinic Acetylcholine Receptor Subtype 4

Xiaoyun Deng<sup>+</sup>,<sup>[a]</sup> Akiko Hatori<sup>+</sup>,<sup>[b]</sup> Zhen Chen,<sup>[a]</sup> Katsushi Kumata,<sup>[b]</sup> Tuo Shao,<sup>[a]</sup> Xiaofei Zhang,<sup>[a]</sup> Tomoteru Yamasaki,<sup>[b]</sup> Kuan Hu,<sup>[b]</sup> Qingzhen Yu,<sup>[a]</sup> Longle Ma,<sup>[a]</sup> Gangqiang Wang,<sup>[c]</sup> Lu Wang,<sup>[a, d]</sup> Yihan Shao,<sup>[e]</sup> Lee Josephson,<sup>[a]</sup> Shaofa Sun,<sup>\*,[c]</sup> Ming-Rong Zhang,<sup>\*,[b]</sup> and Steven Liang<sup>\*,[a]</sup>

Muscarinic acetylcholine receptors (mAChRs) have five distinct subunits ( $M_1$ – $M_5$ ) and are involved in the action of the neurotransmitter acetylcholine in the central and peripheral nervous system. Attributed to the promising clinical efficacy of xanomeline, an  $M_1/M_4$ -preferring agonist, in patients of schizophrenia and Alzheimer's disease,  $M_1$ - or  $M_4$ -selective mAChR modulators have been developed that target the topographically distinct allosteric sites. Herein we report the synthesis and preliminary evaluation of  $^{11}\text{C}$ -labeled positron emission tomography (PET) ligands based on a validated  $M_4$ R positive allosteric modulator VU0467485 (AZ13713945) to facilitate drug discovery. [ $^{11}\text{C}$ ]VU0467485 and two other ligands were prepared in high radiochemical yields (>30%, decay-corrected) with high radiochemical purity (>99%) and high molar activity (>74 GBq  $\mu\text{mol}^{-1}$ ). In vitro autoradiography studies indicated that these three ligands possess moderate-to-high in vitro specific binding to  $M_4$ R. Nevertheless, further physicochemical property optimization is necessary to overcome the challenges associated with limited brain permeability.

Muscarinic acetylcholine receptors (mAChRs), together with nicotinic acetylcholine receptors (nAChRs) constitute the acetylcholine receptor (AChR) families. mAChRs are members of the G protein-coupled receptor superfamily and involved in cognitive, behavior, sensory, motor and autonomic functions.<sup>[1–4]</sup> Five subtypes ( $M_1$ – $M_5$ ) of the muscarinic acetylcholine

receptor (mAChR) have been identified throughout the body in mammals.<sup>[5–8]</sup> In particular, immunoprecipitation studies in rodent brain revealed that  $M_4$  receptor ( $M_4$ R) is abundant in the cerebral cortex, hippocampus, striatum and thalamus, with most density in striatum and lowest in hindbrain, respectively.<sup>[9,10]</sup> A similar distribution of  $M_4$ R in the human brain was also observed.<sup>[10,11]</sup> By autoradiography studies in neurological disorders and neurodegenerative diseases, researchers found that brain sections from Alzheimer's disease (AD) patients showed a significant decrease in  $M_4$ R density in the dentate gyrus, CA4 regions, mediodorsal nucleus, and temporal cortex,<sup>[12–14]</sup> increased levels in striatum and frontal cortex,<sup>[15,16]</sup> but no changes in visual and frontal cortex.<sup>[17]</sup> Postmortem studies with schizophrenia patients showed that significantly decreased expression levels of  $M_4$ R were observed in different brain regions, including anterior cingulate cortex, superior temporal gyrus, prefrontal cortex, hippocampus, caudate, and putamen.<sup>[18–24]</sup> The findings in patients of dementia with Lewy bodies (DLB) revealed that the expression of  $M_4$ R was increased in cortex and claustrum.<sup>[16]</sup> In addition, the  $M_1/M_4$ -preferring agonist xanomeline showed clinical efficacy in schizophrenic and AD patients. By a large-scale, placebo-controlled clinical trial, the observed improvements in Alzheimer's Disease Assessment Scale (ADAS-Cog) and the Clinician's Interview-Based Impression of Change (CIBIC+) following treatment with xanomeline showed that the agonist can be effective for the AD patients in cognitive function improvement.<sup>[25]</sup> Cogni-

[a] Dr. X. Deng,<sup>+</sup> Dr. Z. Chen, Dr. T. Shao, Dr. X. Zhang, Dr. Q. Yu, Dr. L. Ma, Dr. L. Wang, Prof. Dr. L. Josephson, Prof. Dr. S. Liang  
Department of Radiology, Division of Nuclear Medicine and Molecular Imaging, Massachusetts General Hospital and Harvard Medical School, 55 Fruit Street, Boston, MA 02114 (USA)  
E-mail: liang.steven@mg.harvard.edu

[b] Dr. A. Hatori,<sup>+</sup> Dr. K. Kumata, Dr. T. Yamasaki, Dr. K. Hu, Prof. Dr. M.-R. Zhang  
Department of Radiopharmaceuticals Development, National Institute of Radiological Sciences, National Institutes for Quantum and Radiological Science and Technology, Chiba 263-8555 (Japan)  
E-mail: zhang.ming-rong@qst.go.jp

[c] Dr. G. Wang, Prof. Dr. S. Sun  
Hubei Collaborative Innovation Centre for Non-power Nuclear Technology, College of Nuclear Technology & Chemistry and Biology, Hubei University of Science and Technology, Xianning (China)  
E-mail: sunshaofa@hbust.edu.cn

[d] Dr. L. Wang  
Department of Nuclear Medicine and PET/CT-MRI Center, the First Affiliated Hospital of Jinan University & Institute of Molecular and Functional Imaging, Jinan University, Guangzhou 510630 (China)

[e] Prof. Dr. Y. Shao  
Department of Chemistry and Biochemistry, University of Oklahoma, Norman, OK 73019 (USA)

[\*] These authors contributed equally to this work.

 Supporting information and the ORCID identification number(s) for the author(s) of this article can be found under:  
 <https://doi.org/10.1002/cmdc.201800710>

tive improvement for schizophrenia patients provided the evidence that further investigation of xanomeline is worth pursuing as an innovative approach.<sup>[26]</sup> These convincing data resulting from postmortem studies of patients and clinical trials have stimulated the development of therapeutics targeting M<sub>4</sub>R. In particular, the development of M<sub>4</sub>-selective positive allosteric modulators (PAMs) is a novel strategy to overcome the challenges associated with subtype-selective orthosteric muscarinic agonists.<sup>[27,28]</sup> However, at early stage the development of M<sub>4</sub>-selective PAMs was challenging and progressed slowly due to species differences in M<sub>4</sub> PAM potency, challenges in M<sub>4</sub> over M<sub>2</sub> selectivity, P-glycoprotein-mediated efflux, and the lack of chemical diversity.<sup>[27,29–36]</sup> Several M<sub>4</sub> PAMs such as LY2033298, VU10010, ML253, VU0152099, and VU0467154 have been reported in recent years (Figure 1).<sup>[27,29,30,33–35,37–39]</sup> Among these, VU0467485/AZ13713945, a potent and selective

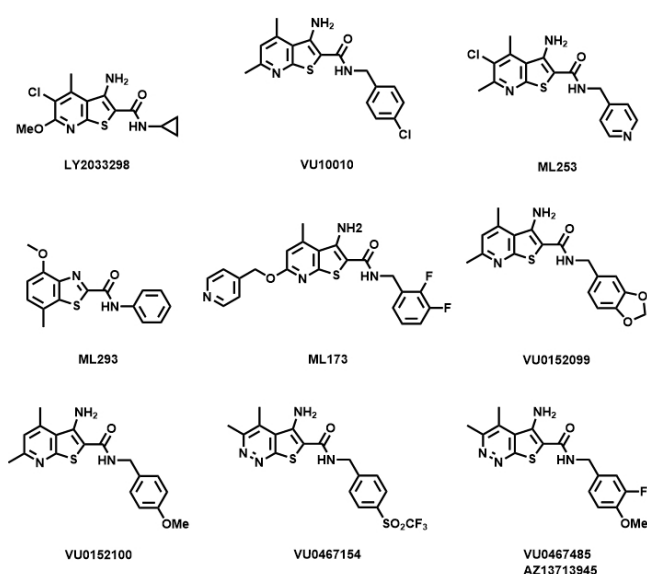
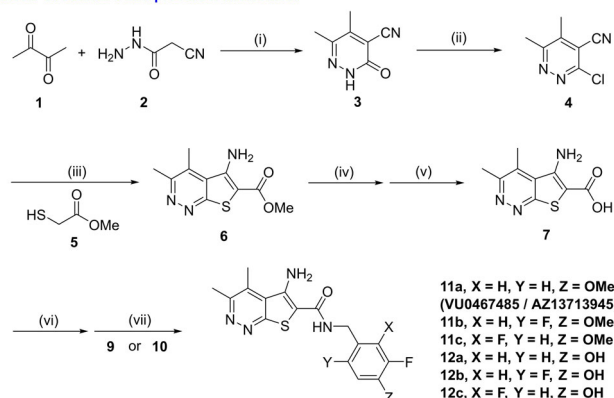


Figure 1. Structures of reported M<sub>4</sub> PAMs.

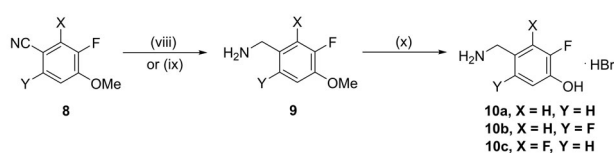
M<sub>4</sub> PAM, represents a major advance in the field with robust efficacy in cross species and behavioral models.<sup>[40]</sup>

Based on the favorable pharmacological and physicochemical characteristics of VU0467485/AZ13713945,<sup>[40]</sup> we hypothesize that this scaffold and its analogues (**11 a–11 c**) may enable the development of a positron emission tomography (PET) ligand targeting M<sub>4</sub>R, and provide a quantitative imaging biomarker for monitoring biochemical and pharmacological process of M<sub>4</sub>R in vivo between normal and disease conditions.<sup>[41–44]</sup> At present, no M<sub>4</sub>R-specific PET ligand is available for human use, which represents an urgent and unmet clinical need. Herein we describe the synthesis of three potent and selective M<sub>4</sub>R PAMs that are amenable for <sup>11</sup>C-labeling and their preliminary evaluation in rodents. In vitro autoradiography studies confirm moderate-to-high binding specificity of these analogues based on VU0467485/AZ13713945 scaffold (with highest levels of specific binding found in [<sup>11</sup>C]11c; also called [<sup>11</sup>C]M<sub>4</sub>R-1023), which may provide an entry point for future M<sub>4</sub>R PET ligand development.

Synthesis of standard and precursor molecules:



Synthesis of Fragment 9 and 10:



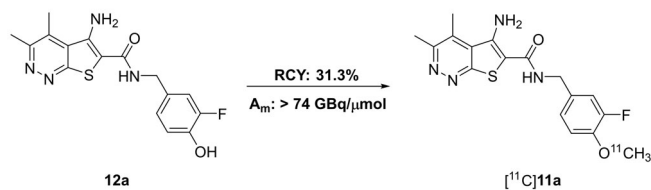
**Scheme 1.** Reagents and conditions: (i) 2 equiv **2**, DMF, 100 °C, 2 h, 37%; (ii) 33 equiv POCl<sub>3</sub>, 1,4-dioxane, reflux, 5 h, 67%; (iii) 1.05 equiv **5**, 1.6 equiv K<sub>2</sub>CO<sub>3</sub>, tBuOH/MeOH, room temperature to 45 °C, 15 h, 98%; (iv) 8 equiv KOH, THF/H<sub>2</sub>O, 60 °C, 4 h; (v) HCl (2 M), 87%; (vi) 1.2 equiv HATU, 3 equiv DIPEA, DMF, room temperature, 10 min; (vii) 2 equiv **9** or **10**, room temperature, 2 h, 85% for **11 a**, 81% for **11 b**, 66% for **11 c**, 41% for **12 a**, 56% for **12 b**, 46% for **12 c**; (viii) 2.0 equiv LiAlH<sub>4</sub>, THF, room temperature, 6 h, 52% for **9 b**; (ix) BH<sub>3</sub>-THF, THF, reflux, 8 h, 53% for **9 c**; (x) HBr (48% aqueous solution), reflux, 5 h, 85% for **10 a**, 50% for **10 b**, 53% for **10 c**; DMF = *N,N*-dimethylformamide; HATU = *O*-(7-azabenzotriazol-1-yl)-*N,N,N',N'*-tetramethyluronium hexafluorophosphate; DIPEA = *N,N*-diisopropylethylamine; THF = tetrahydrofuran.

Three M<sub>4</sub>R PAMs **11 a–c** and their corresponding labeling precursors were synthesized. As summarized in Scheme 1, the cyclization of biacetyl **1** and 2-cyanoacetohydrazide **2** led to intermediate **3** in 37% yield. Phosphorus oxychloride was used to chlorinate compound **3** to obtain the pyridazine chloride **4** in 67% yield. Methyl carboxylate **6** was prepared by cyclization of compound **4** and methyl 2-mercaptoacetate **5** in 98% yield. After hydrolysis, intermediate **6** was converted into the corresponding carboxylic acid **7** in 87% yield. By condensation reactions using HATU and DIPEA, a series of amides **11** and **12** were produced with corresponding amines **8** or **9** in 41–85% yields. It is worth mentioning that sodium carboxylate derivative, obtained by microwave reaction of pyridazine chloride **4** and methyl 2-mercaptoacetate **5** under sodium hydroxide, could also be used as an alternative carboxylate to obtain **11** and **12**. Amine **8 b** was generated by reduction of benzonitrile compound with LiAlH<sub>4</sub> in 52% yield. Because it was not applicable for the preparation of amine **8 c** as one of the fluorine atoms on the arene ring was replaced by hydrogen under LiAlH<sub>4</sub> reduction, BH<sub>3</sub>-THF complex was used to obtain **8 c** in 53% yield. By demethylating the methoxy compound **9** with hydrobromic acid under reflux, we obtained phenolic precursors **10** in 50–85% yields. In all, M<sub>4</sub>R PAMs **11 a–c** and their corresponding precursors **12 a–c** were synthesized in 14–18% and 9–12% overall yields, respectively. The potency of three PAM ligands **11 a–c** was reported,<sup>[40]</sup> which showed human M<sub>4</sub> PAM

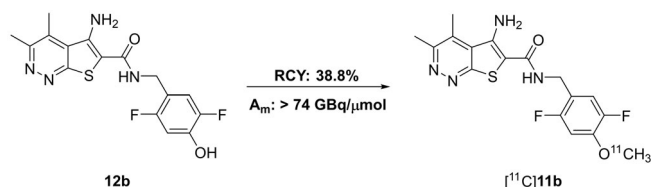
pEC<sub>50</sub> values of 7.10, 7.38 and 7.36, respectively. No off-target subtype binding (M<sub>1</sub>, M<sub>2</sub>, M<sub>3</sub> and M<sub>5</sub>) was observed. Although the potency values of candidate compounds may be not ideal for PET ligand development, as proof of concept, we perform the radiochemistry and preliminary evaluation to study in vitro binding properties and pharmacokinetic profiles, which may provide us a roadmap to guide further SAR studies based on these tool compounds.

As shown in Scheme 2, the methyl ether of M<sub>4</sub>R PAMs was identified as the most accessible labeling site with carbon-

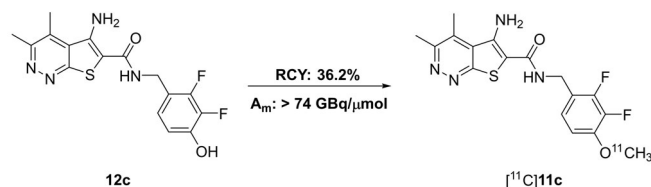
(A) Radiosynthesis of ligand VU0467485 / AZ13713945 (11a)



(B) Radiosynthesis of ligand 11b



(C) Radiosynthesis of ligand 11c

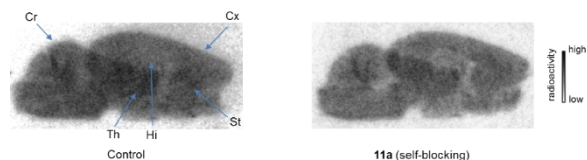


Scheme 2. Radiosynthesis of M<sub>4</sub>R PAM ligands 11 a–c: [<sup>11</sup>C]CH<sub>3</sub>, NaOH, DMF; 80 °C, 5 min.

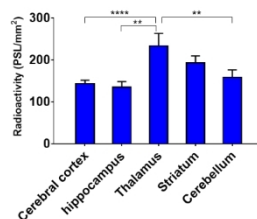
11.<sup>[45]</sup> The synthon [<sup>11</sup>C]CH<sub>3</sub> was transferred into a pre-cooled (–15 to –20 °C) reaction vessel containing precursor 12 a–c, NaOH and anhydrous DMF. After the radioactivity was delivered, the reaction vessel was warmed to 80 °C and maintained for 5 min. The reaction mixture was purified by semi-prep radio-HPLC, and reformulated in a saline solution (3 mL) containing 100 μL of 25% ascorbic acid in sterile water and 100 μL of 20% Tween® 80 in ethanol. The M<sub>4</sub>R PAM ligands [<sup>11</sup>C]11 a–[<sup>11</sup>C]11 c were synthesized in 31–42% radiochemical yield based on [<sup>11</sup>C]CO<sub>2</sub> (decay-corrected). Specifically, starting from 420–600 mCi (15.5–22.2 GBq) of [<sup>11</sup>C]CO<sub>2</sub>, tracers were obtained in 48–63 mCi (1.8–2.3 GBq) at end-of-synthesis (35–40 min synthesis time) with high radiochemical purity (>99%) and high molar activity (>2 Ci μmol<sup>–1</sup>; 74 GBq μmol<sup>–1</sup>). No radiolysis was observed within 90 min.

The binding specificity of [<sup>11</sup>C]VU0467485/[<sup>11</sup>C]AZ13713945 ([<sup>11</sup>C]11 a), [<sup>11</sup>C]11 b and [<sup>11</sup>C]11 c was evaluated by in vitro autoradiography. Representative in vitro autoradiograms of three ligands on sagittal sections of rat brains are shown in Figures 2–

A. In vitro Autoradiography of [<sup>11</sup>C]11a (baseline and blocking)



B. Regional brain distribution



C. Blocking studies

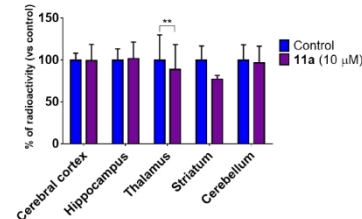
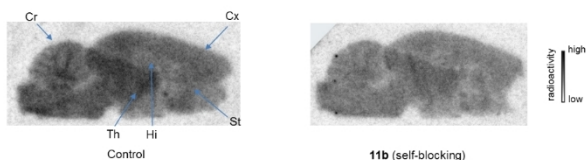


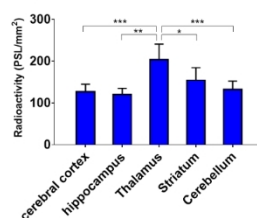
Figure 2. In vitro autoradiography of [<sup>11</sup>C]11 a binding in rat brain sections. (A) Brain sections were treated with [<sup>11</sup>C]11 a in the absence (baseline) or presence of VU0467485/AZ13713945 (11 a; 10 μM). Cr, cerebellum; Cx, cortex; St, striatum; Hi, hippocampus; Th, thalamus. (B) The radioactivity distribution was quantified in regional rat brain. The data are expressed as radioactivity per mm<sup>2</sup> (n = 4). (C) Blocking studies. The data are normalized to percent of radioactivity vs. control (n = 4). Asterisks indicate statistical significance: \*\*p < 0.01 and \*\*\*\*p < 0.0001 vs. control.

4. In the baseline study, the distribution of bound radioactivity was heterogeneous with signal levels in decreasing order of thalamus, striatum, cerebellum, cerebral cortex and hippocampus (Figure 2B, Figure 3B and Figure 4B, respectively). In particular, regional distribution of [<sup>11</sup>C]11 c resembled the most similar expression pattern of M<sub>4</sub>R in the brain as prior reports.<sup>[9,10]</sup> As shown in Figure 2C, quantitative analysis of radioactivity binding in the striatum with VU0467485/AZ13713945 (11 a; 10 μM) showed ~20% reduced binding compared with that of baseline while other regions showed less reduction. In Figure 3C for [<sup>11</sup>C]11 b, self-blocking study in the five tested re-

A. In vitro Autoradiography of [<sup>11</sup>C]11b (baseline and blocking)



B. Regional brain distribution



C. Blocking studies

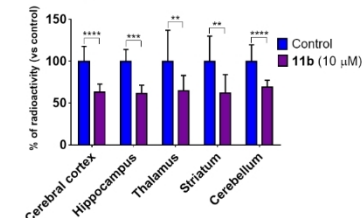
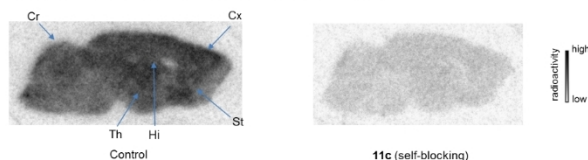
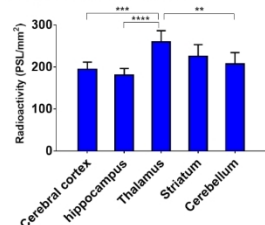


Figure 3. In vitro autoradiography of [<sup>11</sup>C]11 b binding in rat brain sections. (A) Brain sections were treated with [<sup>11</sup>C]11 b in the absence (baseline) or presence of 11 b (10 μM). Cr, cerebellum; Cx, cortex; St, striatum; Hi, hippocampus; Th, thalamus. (B) The radioactivity distribution was quantified in regional rat brain. The data are expressed as radioactivity per mm<sup>2</sup> (n = 4). (C) Blocking studies. The data are normalized to percent of radioactivity vs. control (n = 4). Asterisks indicate statistical significance: \*p < 0.05, \*\*p < 0.01, \*\*\*p < 0.001 and \*\*\*\*p < 0.0001 vs. control.

A. In vitro Autoradiography of [<sup>11</sup>C]11c (baseline and blocking)



B. Regional brain distribution



C. Blocking studies

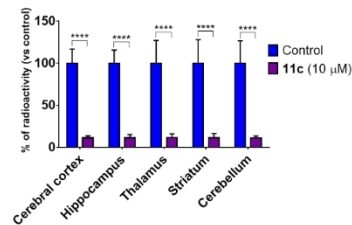


**Figure 4.** In vitro autoradiography of [<sup>11</sup>C]11c binding in rat brain sections. (A) Brain sections were treated with [<sup>11</sup>C]11c in the absence (baseline) or presence of 11c (10 µM). Cr, cerebellum; Cx, cortex; St, striatum; Hi, hippocampus; Th, thalamus. (B) The radioactivity distribution was quantified in regional rat brain. The data are expressed as radioactivity per mm<sup>2</sup> (n=4). (C) Blocking studies. The data are normalized to percent of radioactivity vs. control (n=4). Asterisks indicate statistical significance: \*\*p < 0.01, \*\*\*p < 0.001, and \*\*\*\*p < 0.0001 vs. control.

gions showed ~30–40% reduced binding compared with that of baseline. In Figure 4C, [<sup>11</sup>C]11c showed highest level of specific binding among three ligands, as ~90% reduced binding was observed in the five tested regions. These encouraging results prompted us to perform in vivo evaluation of [<sup>11</sup>C]11c in PET studies.

Dynamic PET acquisitions (0–60 min) were conducted with [<sup>11</sup>C]11c in Sprague–Dawley rats. Representative PET images of [<sup>11</sup>C]11c (sagittal and coronal, summed 0–60 min) and time-activity curves of five brain regions at baseline conditions are shown in Figure 5. The potential M<sub>4</sub>R ligand [<sup>11</sup>C]11c showed limited brain uptake (~0.4 SUV peak uptake) with a heterogeneous distribution in decreasing order of cerebellum, cerebral cortex, hippocampus and striatum. Pretreatment with unradiolabeled M<sub>4</sub>R PAM VU0467485/AZ13713945 (**11a**; 1 mg kg<sup>-1</sup>) failed to show the substantial difference of [<sup>11</sup>C]11c uptake in the brain relative to baseline conditions (Figure S1, Supporting

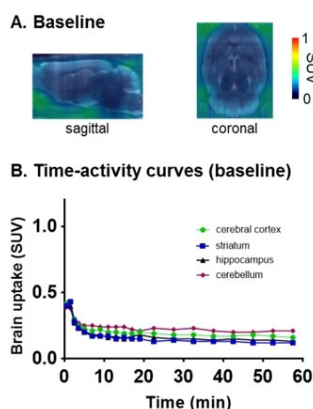


**Figure 5.** PET/MRI fused images of [<sup>11</sup>C]11c in rat brain: (A) baseline and (B) time-activity curves in different brain regions at baseline.

Information). A possible explanation was as follows: While the ligand of this type showed reasonable CNS penetration in vitro and in vivo (exemplified in **11a** with efflux ratio of 1.4 in MDCK/MDR1 assay; total brain/total plasma, K<sub>p</sub> of 0.31 and unbound brain/unbound plasma, K<sub>p,uu</sub> of 0.37 in Sprague–Dawley rats),<sup>[40]</sup> the PAM can be functionally potent, but is a possible weak binder due to cooperativity, leading to greater chance of nonspecific binding.

We have efficiently synthesized three PAMs targeting M<sub>4</sub>R and their corresponding labeling precursors. The <sup>11</sup>C-labeling experiments were carried out in excellent radiochemical yield, high radiochemical purity and high molar activity. In vitro autoradiography studies confirmed moderate-to-high specific binding of all these M<sub>4</sub>R ligands. While [<sup>11</sup>C]11c (also called [<sup>11</sup>C]M<sub>4</sub>R-1023) is not likely advanced for in vivo mapping of M<sub>4</sub>R due to limited brain permeability, in vitro high specific binding showed a promising chemotype for further M<sub>4</sub>R PET ligand development. Further in-depth pharmacokinetic studies are necessary to test Pgp/Bcrp brain efflux accountability in cross species studies and to facilitate new tier design with improved brain permeability.

## Experimental Section

The general experimental section was described previously<sup>[46]</sup> with minor modification as follows: All the chemicals employed in the syntheses were purchased from commercial vendors and used without further purification. Thin-layer chromatography (TLC) was conducted with 0.25 mm silica gel plates (<sup>60</sup>F<sub>254</sub>) and visualized by exposure to UV light (254 nm) or stained with potassium permanganate. Flash column chromatography was performed using silica gel (particle size 0.040–0.063 mm). Nuclear magnetic resonance (NMR) spectra were obtained on a Bruker spectrometer 300 MHz. Chemical shifts (δ) are reported in ppm and coupling constants are reported in Hertz. The multiplicities are abbreviated as follows: s = singlet, d = doublet, t = triplet, q = quartet, quint = quintet, sext = sextet, sept = septet, m = multiplet, br = broad signal, dd = doublet of doublets. For LC–MS/MS measurements, the ionization method is ESI using Agilent 6430 Triple Quad LC–MS. The animal experiments were approved by the Institutional Animal Care and Use Committee of Massachusetts General Hospital or the Animal Ethics Committee at the National Institutes for Quantum and Radiological Science and Technology, National Institute of Radiological Sciences. Sprague–Dawley rats (male, 7 weeks old) were used for PET imaging studies.

**General procedure for the condensation reaction:** A mixture of compound **7** (0.2 mmol), *N,N*-diisopropylethylamine (0.6 mmol, 3 equiv) and *O*-(7-azabenzotriazole-1-yl)-1,1,3,3-tetramethyluronium hexafluorophosphate (HATU, 0.24 mmol, 1.2 equiv) in DMF (1 mL) was allowed to stir at ambient temperature for 10 min; then **9a–10c** (0.4 mmol, 2 equiv) in DMF (1 mL) was added. After stirring for an additional 2 h, the mixture was purified by chromatography on silica gel, elution being carried out with ethyl acetate. Compounds **11a–12c** were prepared in 41–85% yields.

**5-amino-*N*-(3-fluoro-4-methoxybenzyl)-3,4-dimethylthieno[2,3-*c*]pyridazine-6-carboxamide (VU0467485/AZ13713945; **11a**):** According to the general procedure for the condensation reaction, compound **11a** was prepared in 85% yield as a yellow solid. <sup>1</sup>H NMR (300 MHz, DMSO): δ = 8.60 (t, *J* = 5.8 Hz, 1H), 7.15–6.96 (m, 5H), 4.35 (d, *J* = 5.9 Hz, 2H), 3.80 (s, 3H), 2.70 (s, 3H), 2.69 ppm (s,

3H);  $^{13}\text{C}$  NMR (75 MHz, DMSO):  $\delta$  = 165.15 (s), 160.21 (s), 154.97 (s), 151.69 (d,  $J$  = 243.0 Hz), 146.79 (s), 146.40 (d,  $J$  = 10.3 Hz), 133.06 (s), 132.98 (s), 127.45 (s), 124.00 (s), 115.44 (d,  $J$  = 18.0 Hz), 114.15 (s), 102.90 (s), 56.45 (s), 42.10 (s), 20.19 (s), 15.01 ppm (s).

**5-amino-*N*-(2,5-difluoro-4-methoxybenzyl)-3,4-dimethylthieno[2,3-*c*]pyridazine-6-carboxamide (11 b):** According to the general procedure for the condensation reaction, compound **11 b** was prepared in 81% yield as a yellow solid. Melting point: 235–237 °C;  $^1\text{H}$  NMR (300 MHz, DMSO):  $\delta$  = 8.57 (t,  $J$  = 5.6 Hz, 1H), 7.14 (ddd,  $J$  = 23.0, 11.6, 7.1 Hz, 2H), 6.94 (s, 2H), 4.38 (d,  $J$  = 5.6 Hz, 2H), 3.82 (s, 3H), 2.70 (s, 3H), 2.68 ppm (s, 3H);  $^{13}\text{C}$  NMR (75 MHz, DMSO):  $\delta$  = 165.27 (s), 160.23 (s), 156.21 (dd,  $J$  = 241.0, 2.2 Hz), 154.99 (s), 148.03 (dd,  $J$  = 239.7, 2.8 Hz), 147.33 (dd,  $J$  = 12.3, 10.7 Hz), 146.92 (s), 133.07 (s), 127.35 (s), 117.94 (dd,  $J$  = 17.7, 5.9 Hz), 116.32 (dd,  $J$  = 20.7, 6.3 Hz), 102.62 (s), 102.27 (d,  $J$  = 1.6 Hz), 56.93 (s), 36.08 (s), 20.19 (s), 15.01 ppm (s).

**5-amino-*N*-(2,3-difluoro-4-methoxybenzyl)-3,4-dimethylthieno[2,3-*c*]pyridazine-6-carboxamide (11 c):** According to the general procedure for the condensation reaction, compound **11 c** was prepared in 66% yield as a yellow solid. Melting point: 217–219 °C;  $^1\text{H}$  NMR (300 MHz, DMSO):  $\delta$  = 8.62 (t,  $J$  = 5.6 Hz, 1H), 7.16–6.95 (m, 4H), 4.42 (d,  $J$  = 5.6 Hz, 2H), 3.84 (s, 3H), 2.71 (s, 3H), 2.69 ppm (s, 3H);  $^{13}\text{C}$  NMR (75 MHz, DMSO):  $\delta$  = 165.20 (s), 160.23 (s), 154.94 (s), 148.85 (dd,  $J$  = 245.0, 10.4 Hz), 147.91 (dd,  $J$  = 7.7, 3.0 Hz), 146.89 (s), 140.32 (dd,  $J$  = 245.0, 14.3 Hz), 133.29 (s), 127.49 (s), 123.89 (dd,  $J$  = 5.1, 4.4 Hz), 120.08 (dd,  $J$  = 12.3, 1.3 Hz), 109.27 (d,  $J$  = 3.2 Hz), 102.76 (s), 56.96 (s), 36.24 (s), 20.12 (s), 15.03 ppm (s).

**5-amino-*N*-(3-fluoro-4-hydroxybenzyl)-3,4-dimethylthieno[2,3-*c*]pyridazine-6-carboxamide (12 a):** According to the general procedure for the condensation reaction, compound **12 a** was prepared in 41% yield as a yellow solid. Melting point: 188–190 °C;  $^1\text{H}$  NMR (300 MHz, DMSO):  $\delta$  = 9.70 (s, 1H), 8.56 (t,  $J$  = 5.9 Hz, 1H), 7.07 (dd,  $J$  = 12.3, 1.3 Hz, 1H), 6.98–6.84 (m, 4H), 4.31 (d,  $J$  = 5.9 Hz, 2H), 2.70 (s, 3H), 2.68 ppm (s, 3H);  $^{13}\text{C}$  NMR (75 MHz, DMSO):  $\delta$  = 165.10 (s), 160.20 (s), 154.95 (s), 151.18 (d,  $J$  = 240.5 Hz), 146.74 (s), 144.05 (d,  $J$  = 12.2 Hz), 132.99 (s), 131.42 (d,  $J$  = 5.8 Hz), 127.41 (s), 124.00 (d,  $J$  = 2.9 Hz), 117.95 (d,  $J$  = 3.0 Hz), 115.63 (d,  $J$  = 18.5 Hz), 102.98 (s), 42.09 (s), 20.19 (s), 15.00 ppm (s); MS:  $m/z$   $[M + 1]^+$  = 347.

**5-amino-*N*-(2,5-difluoro-4-hydroxybenzyl)-3,4-dimethylthieno[2,3-*c*]pyridazine-6-carboxamide (12 b):** According to the general procedure for the condensation reaction, compound **12 b** was prepared in 56% yield as a yellow solid.  $^1\text{H}$  NMR (300 MHz, DMSO):  $\delta$  = 10.25 (s, 1H), 8.53 (t,  $J$  = 5.6 Hz, 1H), 7.15–6.70 (m, 4H), 4.35 (d,  $J$  = 5.6 Hz, 2H), 2.69 (s, 3H), 2.68 ppm (s, 3H);  $^{13}\text{C}$  NMR (75 MHz, DMSO):  $\delta$  = 165.23 (s), 160.22 (s), 155.98 (dd,  $J$  = 240.5, 1.9 Hz), 154.94 (s), 147.77 (dd,  $J$  = 236.6, 2.5 Hz), 146.86 (s), 145.16 (dd,  $J$  = 14.3, 11.8 Hz), 133.05 (s), 127.35 (s), 116.79 (dd,  $J$  = 6.0, 4.0 Hz), 116.53 (dd,  $J$  = 7.3, 6.1 Hz), 105.06 (dd,  $J$  = 26.4, 3.1 Hz), 102.71 (s), 36.09 (s), 20.16 (s), 15.00 ppm (s); MS:  $m/z$   $[M + 1]^+$  = 365.

**5-amino-*N*-(2,3-difluoro-4-hydroxybenzyl)-3,4-dimethylthieno[2,3-*c*]pyridazine-6-carboxamide (12 c):** According to the general procedure for the condensation reaction, compound **12 c** was prepared in 81% yield as an orange red solid. Melting point: 245–247 °C;  $^1\text{H}$  NMR (300 MHz, DMSO):  $\delta$  = 10.26 (s, 1H), 8.56 (t,  $J$  = 5.5 Hz, 1H), 7.02–6.70 (m, 4H), 4.39 (d,  $J$  = 5.5 Hz, 2H), 2.70 (s, 3H), 2.69 ppm (s, 3H);  $^{13}\text{C}$  NMR (75 MHz, DMSO):  $\delta$  = 165.18 (s), 160.23 (s), 154.97 (s), 149.24 (dd,  $J$  = 244.5, 10.6 Hz), 146.85 (s), 145.91 (dd,  $J$  = 9.0, 2.8 Hz), 139.97 (dd,  $J$  = 242.1, 14.2 Hz), 133.08 (s), 127.37 (s), 123.81 (dd,  $J$  = 5.3, 4.2 Hz), 118.12 (dd,  $J$  = 12.2, 1.4 Hz), 113.00 (dd,

$J$  = 3.1, 1.5 Hz), 102.76 (s), 36.17 (s), 20.18 (s), 15.01 ppm (s); MS:  $m/z$   $[M + 1]^+$  = 365.

**General procedure for  $^{11}\text{C}$ -methylation:** The general procedure for  $^{11}\text{C}$ -labeling was described previously<sup>[46]</sup> with minor modification in this work. Briefly, [ $^{11}\text{C}$ ]methyl iodide ([ $^{11}\text{C}$ ]CH<sub>3</sub>I) was synthesized from cyclotron-produced [ $^{11}\text{C}$ ]CO<sub>2</sub>, which was produced by  $^{14}\text{N}(p,\alpha)^{11}\text{C}$  nuclear reaction. Briefly, [ $^{11}\text{C}$ ]CO<sub>2</sub> was bubbled into a solution of LiAlH<sub>4</sub> (0.4 M in THF, 300  $\mu\text{L}$ ). After evaporation, the remaining reaction mixture was treated with hydroiodic acid (57% aqueous solution, 300  $\mu\text{L}$ ). The resulting [ $^{11}\text{C}$ ]CH<sub>3</sub>I was transferred under helium gas with heating into a pre-cooled (–15 to –20 °C) reaction vessel containing precursor (1.0 mg), NaOH (6.0  $\mu\text{L}$ , 0.5 M) and anhydrous DMF (300  $\mu\text{L}$ ). After the radioactivity reached a plateau during transfer, the reaction vessel was warmed to 80 °C and maintained for 5 min. CH<sub>3</sub>CN/H<sub>2</sub>O + 0.1% Et<sub>3</sub>N (0.5 mL) was added to the reaction mixture, which was then injected to a semi-preparative HPLC system. HPLC purification was completed on a Capcell Pak UG80 C<sub>18</sub> column (10 mm ID  $\times$  250 mm) using a mobile phase of CH<sub>3</sub>CN/H<sub>2</sub>O + 0.1% Et<sub>3</sub>N. The radioactive fraction corresponding to the desired product was collected in a sterile flask, evaporated to dryness in vacuo, and reformulated in a saline solution (3 mL) containing 100  $\mu\text{L}$  of 25% ascorbic acid in sterile water and 100  $\mu\text{L}$  of 20% Tween<sup>®</sup> 80 in ethanol. Radiochemical and chemical purity were measured by analytical HPLC (Capcell Pak UG80 C<sub>18</sub>, 4.6 mm ID  $\times$  250 mm, UV at 254 nm; CH<sub>3</sub>CN/H<sub>2</sub>O + 0.1% Et<sub>3</sub>N at a flow rate of 1.0 mL min<sup>–1</sup>). The identity of [ $^{11}\text{C}$ ]11 a–c was confirmed by the co-injection with unlabeled 11 a–c.

**5-amino-*N*-(3-fluoro-4-[ $^{11}\text{C}$ ]methoxybenzyl)-3,4-dimethylthieno[2,3-*c*]pyridazine-6-carboxamide ([ $^{11}\text{C}$ ]VU0467485/[ $^{11}\text{C}$ ]AZ13713945/[ $^{11}\text{C}$ ]11 a):** According to the general procedure<sup>[46]</sup> for the  $^{11}\text{C}$ -methylation, the retention time for [ $^{11}\text{C}$ ]11 a was 12.0 min. The synthesis time was ~40 min from end-of-bombardment. HPLC purification was completed on a Capcell Pak UG80 C<sub>18</sub> column (10 mm ID  $\times$  250 mm) using a mobile phase of CH<sub>3</sub>CN/H<sub>2</sub>O (v/v, 4:6) + 0.1% Et<sub>3</sub>N at a flow rate of 4.0 mL min<sup>–1</sup>. Radiochemical and chemical purity were measured by analytical HPLC (Capcell Pak UG80 C<sub>18</sub>, 4.6 mm ID  $\times$  250 mm, UV at 254 nm; CH<sub>3</sub>CN/H<sub>2</sub>O (v/v, 4:6) + 0.1% Et<sub>3</sub>N at a flow rate of 1.0 mL min<sup>–1</sup>). Radiochemical yield was 31.3% decay-corrected based on [ $^{11}\text{C}$ ]CO<sub>2</sub> with > 99% radiochemical purity and greater than 2 Ci  $\mu\text{mol}^{-1}$  molar activity.

**5-amino-*N*-(2,5-difluoro-4-[ $^{11}\text{C}$ ]methoxybenzyl)-3,4-dimethylthieno[2,3-*c*]pyridazine-6-carboxamide ([ $^{11}\text{C}$ ]11 b):** According to the general procedure<sup>[46]</sup> for the  $^{11}\text{C}$ -methylation, the retention time for [ $^{11}\text{C}$ ]11 b was 8.1 min. The synthesis time was ~35 min from end-of-bombardment. HPLC purification was completed on a Capcell Pak UG80 C<sub>18</sub> column (10 mm ID  $\times$  250 mm) using a mobile phase of CH<sub>3</sub>CN/H<sub>2</sub>O (v/v, 45:55) + 0.1% Et<sub>3</sub>N at a flow rate of 5.0 mL min<sup>–1</sup>. Radiochemical and chemical purity were measured by analytical HPLC (Capcell Pak UG80 C<sub>18</sub>, 4.6 mm ID  $\times$  250 mm, UV at 254 nm; CH<sub>3</sub>CN/H<sub>2</sub>O (v/v, 45:55) + 0.1% Et<sub>3</sub>N at a flow rate of 1.0 mL min<sup>–1</sup>). Radiochemical yield was 38.8% decay-corrected based on [ $^{11}\text{C}$ ]CO<sub>2</sub> with > 99% radiochemical purity and greater than 2 Ci  $\mu\text{mol}^{-1}$  molar activity.

**5-amino-*N*-(2,3-difluoro-4-[ $^{11}\text{C}$ ]methoxybenzyl)-3,4-dimethylthieno[2,3-*c*]pyridazine-6-carboxamide ([ $^{11}\text{C}$ ]11 c):** According to the general procedure<sup>[46]</sup> for the  $^{11}\text{C}$ -methylation, the retention time for [ $^{11}\text{C}$ ]11 c was 8.5 min. The synthesis time was ~35 min from end-of-bombardment. HPLC purification was completed on a Capcell Pak UG80 C<sub>18</sub> column (10 mm ID  $\times$  250 mm) using a mobile phase of CH<sub>3</sub>CN/H<sub>2</sub>O (v/v, 45:55) + 0.1% Et<sub>3</sub>N at a flow rate of 5.0 mL min<sup>–1</sup>. Radiochemical and chemical purity were measured by analytical

HPLC (Capcell Pak UG80 C<sub>18</sub>, 4.6 mm ID×250 mm, UV at 254 nm; CH<sub>3</sub>CN/H<sub>2</sub>O (v/v, 45:55) + 0.1% Et<sub>3</sub>N at a flow rate of 1.0 mL min<sup>-1</sup>). Radiochemical yield was 41.3% decay-corrected based on [<sup>11</sup>C]CO<sub>2</sub> with >99% radiochemical purity and greater than 2 Ci μmol<sup>-1</sup> molar activity.

**In vitro autoradiography:** The general procedure for in vitro autoradiography was described previously<sup>[46]</sup> with minor modification in this work. Briefly, rat brain was cut into 20 μm sections and stored at -80 °C until they were used for experiment. The rat brain sections were preincubated with Tris-HCl buffer (pH 7.4, 50 mM), MgCl<sub>2</sub> (1.2 mM), and CaCl<sub>2</sub> (2 mM) solution for 20 min at ambient temperature, followed by incubation with [<sup>11</sup>C]11 (37 MBq/200 mL) for 30 min at ambient temperature. For blocking studies, unlabeled 11 (10 μM) was added to incubation solution in advance to determine the specificity of radioligand binding. After incubation, brain sections were washed with Tris buffer two times for 2 min and dipped in cold distilled water for 10 s. The brain sections were dried with cold air, then placed on imaging plates (BASMS2025, GE Healthcare, NJ, USA) for 60 min. Autoradiograms were obtained and ROIs were carefully drawn with the reference of naked-eye observation. Radioactivity was expressed as photostimulated luminescence values per unit area (PSL/mm<sup>2</sup>) and measured by a Bio-Imaging analyzer system (BAS5000, Fujifilm).

**PET imaging studies:** The general procedure for PET studies was described previously<sup>[46]</sup> with minor modification in this work. Briefly, PET scans were carried out by an Inveon PET scanner (Siemens Medical Solutions, Knoxville, TN, USA). Sprague-Dawley rats were kept under anesthesia with 1–2% (v/v) isoflurane during the scan. The [<sup>11</sup>C]11c (~1 mCi/100 μL) was injected via a preinstalled catheter via the tail vein. A dynamic scan was acquired for 60 min in three-dimensional list mode. For pretreatment studies, unlabeled VU0467485/AZ13713945 (11a; 1 mg kg<sup>-1</sup>) dissolved in 300 μL saline containing 10% ethanol and 5% Tween® 80 was injected at 5 min via the pre-embedded tail vein catheter before the injection of [<sup>11</sup>C]11c. The PET dynamic images were reconstructed using ASIPro VW software (Analysis Tools and System Setup/Diagnostics Tool, Siemens Medical Solutions). Volumes of interest, including hippocampus, cerebral cortex, cerebellum and striatum were placed using ASIPro VM. The radioactivity was decay-corrected and expressed as the standardized uptake value. SUV = (radioactivity per mL tissue)/(injected radioactivity) × body weight.

## Acknowledgements

We thank Professor Thomas J. Brady (Nuclear Medicine and Molecular Imaging, Radiology, MGH and Harvard Medical School) for helpful discussions.

## Conflict of interest

The authors declare no conflict of interest.

**Keywords:** carbon-11 • muscarinic acetylcholine receptor subtype 4 • positive allosteric modulator • positron emission tomography • VU0467485/AZ13713945

[1] J. Wess, *Crit. Rev. Neurobiol.* **1996**, *10*, 69.

[2] L. A. Volpicelli, A. I. Levey, *Prog. Brain Res.* **2004**, *145*, 59.

[3] M. Ishii, Y. Kurachi, *Curr. Pharm. Des.* **2006**, *12*, 3573.

- [4] P. Abrams, K. E. Andersson, J. J. Buccafusco, C. Chapple, W. C. De Groat, A. D. Fryer, G. Kay, A. Laties, N. M. Nathanson, P. J. Pasricha, *Br. J. Pharmacol.* **2006**, *148*, 565.
- [5] M. P. Caulfield, N. J. Birdsall, *Pharmacol. Rev.* **1998**, *50*, 279.
- [6] T. Bonner, N. Buckley, A. Young, M. Brann, *Science* **1987**, *237*, 527.
- [7] T. I. Bonner, A. C. Young, M. R. Bran, N. J. Buckley, *Neuron* **1988**, *1*, 403.
- [8] E. Hulme, Z. Lu, J. Saldanha, M. Bee, *Biochem. Soc. Trans.* **2003**, *31*, 29.
- [9] A. Levey, C. Kitt, W. Simonds, D. Price, M. Brann, *J. Neurosci.* **1991**, *11*, 3218.
- [10] A. I. Levey, *Life Sci.* **1993**, *52*, 441.
- [11] M. Piggott, J. Owens, J. O'Brien, S. Paling, D. Wyper, J. Fenwick, M. Johnson, R. Perry, E. Perry, *J. Chem. Neuroanat.* **2002**, *24*, 211.
- [12] E. Mulugeta, E. Karlsson, A. Islam, R. Kalaria, H. Mangat, B. Winblad, A. Adem, *Brain Res.* **2003**, *960*, 259.
- [13] N. M. Warren, M. A. Piggott, A. J. Lees, D. J. Burn, *J. Neuropathol. Exp. Neurol.* **2007**, *66*, 399.
- [14] K. Shiozaki, E. Iseki, H. Uchiyama, Y. Watanabe, T. Haga, K. Kameyama, T. Ikeda, T. Yamamoto, K. Kosaka, *J. Neurol. Neurosurg. Psychiatry* **1999**, *67*, 209.
- [15] D. D. Flynn, G. Ferrari-DiLeo, A. I. Levey, D. C. Mash, *Life Sci.* **1995**, *56*, 869.
- [16] M. A. Piggott, J. Owens, J. O'Brien, S. Colloby, J. Fenwick, D. Wyper, E. Jaros, M. Johnson, R. H. Perry, E. K. Perry, *J. Chem. Neuroanat.* **2003**, *25*, 161.
- [17] R. Rodríguez-Puertas, J. Pascual, T. Vilaró, Á. Pazos, *Synapse* **1997**, *26*, 341.
- [18] T. Raedler, F. Bymaster, R. Tandon, D. Copolov, B. Dean, *Mol. Psychiatry* **2007**, *12*, 232.
- [19] Z. Katerina, K. Andrew, M. Filomena, X.-F. Huang, *Neuropsychopharmacology* **2004**, *29*, 619.
- [20] C. Deng, X. F. Huang, *J. Neurosci. Res.* **2005**, *81*, 883.
- [21] J. M. Crook, E. Tomaskovic-Crook, D. L. Copolov, B. Dean, *Am. J. Psychiatry* **2001**, *158*, 918.
- [22] J. M. Crook, E. Tomaskovic-Crook, D. L. Copolov, B. Dean, *Biol. Psychiatry* **2000**, *48*, 381.
- [23] J. M. Crook, B. Dean, G. Pavey, D. Copolov, *Life Sci.* **1999**, *64*, 1761.
- [24] E. Scarr, S. Sundram, D. Keriakous, B. Dean, *Biol. Psychiatry* **2007**, *61*, 1161.
- [25] N. C. Bodick, W. W. Offen, A. I. Levey, N. R. Cutler, S. G. Gauthier, A. Satlin, H. E. Shannon, G. D. Tollefson, K. Rasmussen, F. P. Bymaster, *Arch. Neurol.* **1997**, *54*, 465.
- [26] A. Shekhar, W. Z. Potter, J. Lightfoot, J. Lienemann, D. Pharm, S. Dubé, C. Mallinckrodt, F. P. Bymaster, D. L. McKinzie, C. C. Felder, *Am. J. Psychiatry* **2008**, *165*, 1033.
- [27] M. Bubser, T. M. Bridges, D. Dencker, R. W. Gould, M. Grannan, M. J. Noetzel, A. Lamsal, C. M. Niswender, J. S. Daniels, M. S. Poslusney, *ACS Chem. Neurosci.* **2014**, *5*, 920.
- [28] C. W. Lindsley, K. A. Emmitte, C. R. Hopkins, T. M. Bridges, K. J. Gregory, C. M. Niswender, P. J. Conn, *Chem. Rev.* **2016**, *116*, 6707.
- [29] W. Chan, D. McKinzie, S. Bose, S. Mitchell, J. Witkin, R. Thompson, A. Christopoulos, S. Lazareno, N. Birdsall, F. Bymaster, *Proc. Natl. Acad. Sci. USA* **2008**, *105*, 10978.
- [30] A. E. Brady, C. K. Jones, T. M. Bridges, J. P. Kennedy, A. D. Thompson, J. U. Heiman, M. L. Breining, P. R. Gentry, H. Yin, S. B. Jadhav, *J. Pharmacol. Exp. Ther.* **2008**, *327*, 941.
- [31] K. Leach, R. E. Loiacono, C. C. Felder, D. L. McKinzie, A. Mogg, D. B. Shaw, P. M. Sexton, A. Christopoulos, *Neuropsychopharmacology* **2010**, *35*, 855.
- [32] N. E. Byun, M. Grannan, M. Bubser, R. L. Barry, A. Thompson, J. Rosanelli, R. Gowrishankar, N. D. Kelm, S. Damon, T. M. Bridges, *Neuropsychopharmacology* **2014**, *39*, 1578.
- [33] M. R. Wood, M. J. Noetzel, M. S. Poslusney, B. J. Melancon, J. C. Tarr, A. Lamsal, S. Chang, V. B. Luscombe, R. L. Weiner, H. P. Cho, *Bioorg. Med. Chem. Lett.* **2017**, *27*, 171.
- [34] U. Le, B. J. Melancon, T. M. Bridges, P. N. Vinson, T. J. Utley, A. Lamsal, A. L. Rodriguez, D. Venable, D. J. Sheffler, C. K. Jones, *Bioorg. Med. Chem. Lett.* **2013**, *23*, 346.
- [35] J. M. Salovich, P. N. Vinson, D. J. Sheffler, A. Lamsal, T. J. Utley, A. L. Blobaum, T. M. Bridges, U. Le, C. K. Jones, M. R. Wood, *Bioorg. Med. Chem. Lett.* **2012**, *22*, 5084.

- [36] M. R. Wood, M. J. Noetzel, J. L. Engers, K. A. Bollinger, B. J. Melancon, J. C. Tarr, C. Han, M. West, A. R. Gregro, A. Lamsal, *Bioorg. Med. Chem. Lett.* **2016**, *26*, 3029.
- [37] J. K. Shirey, Z. Xiang, D. Orton, A. E. Brady, K. A. Johnson, R. Williams, J. E. Ayala, A. L. Rodriguez, J. Wess, D. Weaver, *Nat. Chem. Biol.* **2008**, *4*, 42.
- [38] T. Huynh, C. Valant, I. T. Crosby, P. M. Sexton, A. Christopoulos, B. Capuano, *J. Med. Chem.* **2013**, *56*, 8196.
- [39] J. P. Kennedy, T. M. Bridges, P. R. Gentry, J. T. Brogan, A. S. Kane, C. K. Jones, A. E. Brady, J. K. Shirey, P. J. Conn, C. W. Lindsley, *ChemMedChem* **2009**, *4*, 1600.
- [40] M. R. Wood, M. J. Noetzel, B. J. Melancon, M. S. Poslusney, K. D. Nance, M. A. Hurtado, V. B. Luscombe, R. L. Weiner, A. L. Rodriguez, A. Lamsal, *ACS Med. Chem. Lett.* **2017**, *8*, 233.
- [41] J. S. Fowler, A. P. Wolf, *Acc. Chem. Res.* **1997**, *30*, 181.
- [42] M. E. Phelps, *Proc. Natl. Acad. Sci. USA* **2000**, *97*, 9226.
- [43] J. K. Willmann, N. Van Bruggen, L. M. Dinkelborg, S. S. Gambhir, *Nat. Rev. Drug Discovery* **2008**, *7*, 591.
- [44] S. M. Ametamey, M. Honer, P. A. Schubiger, *Chem. Rev.* **2008**, *108*, 1501.
- [45] X. Deng, J. Rong, L. Wang, N. Vasdev, L. Zhang, L. Josephson, S. Liang, *Angew. Chem. Int. Ed.* **2018**, DOI: <https://doi.org/10.1002/anie.201805501>.
- [46] X. Zhang, K. Kumata, T. Yamasaki, R. Cheng, A. Hatori, L. Ma, Y. Zhang, L. Wang, H. J. Kang, D. J. Sheffler, N. D. P. Cosford, M.-R. Zhang, S. H. Liang, *ACS Chem. Neurosci.* **2017**, *8*, 1937.

Manuscript received: November 5, 2018

Accepted manuscript online: ■ ■ ■ ■, 0000

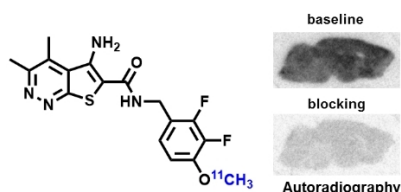
Version of record online: ■ ■ ■ ■, 0000

## COMMUNICATIONS

X. Deng, A. Hatori, Z. Chen, K. Kumata, T. Shao, X. Zhang, T. Yamasaki, K. Hu, Q. Yu, L. Ma, G. Wang, L. Wang, Y. Shao, L. Josephson, S. Sun,\* M.-R. Zhang,\* S. Liang\*



**Synthesis and Preliminary Evaluation of  $^{11}\text{C}$ -Labeled VU0467485/AZ13713945 and Its Analogues for Imaging Muscarinic Acetylcholine Receptor Subtype 4**



**Carbon-11 footprint:** A validated  $\text{M}_4\text{R}$  positive allosteric modulator VU0467485 (AZ13713945) was evaluated as a pre-clinical candidate. A series of  $^{11}\text{C}$ -labeled positron emission tomography (PET) ligands based on VU0467485 were synthesized and preliminarily evaluated. In vitro autoradiography studies indicated that these PET ligands possess moderate-to-high in vitro specific binding to  $\text{M}_4\text{R}$ . Nevertheless, further optimization is necessary to improve brain permeability.